# Evaluation and development of heat transfer model for supercritical water flowing in 2 × 2 rod bundles with spacer grid

Meng Zhao, Fangnian Wang*, Aurelian Florin Badea

*Institute for Applied Thermofluidics (IATF), Karlsruhe Institute of Technologies (KIT), Karlsruhe 76131, Germany*

ARTICLE INFO

*Keywords:*
Supercritical water
heat transfer model
spacer effect
enhancement heat transfer

ABSTRACT

Supercritical water has excellent heat transfer abilities that allows higher power density and smaller structure in power plants. However, due to the large variation of the fluid thermal-physical properties near pseudo-critical point, heat transfer to supercritical water shows abnormal behavior at certain points. Thus, an accurate prediction model of heat transfer to fluid is very important to the supercritical energy system design. The present studies performed an experiment of 2 × 2 rod bundles with spacer effect at supercritical pressure and more than 5000 data pointes were obtained. A thorough analysis and assessment of the heat transfer models was carried out, to give an insight into the characters of the present heat transfer models for the fully-developed flow and spacer grid influenced flow. The result shows that the Watts-Chou correlation can predict the so-called normal heat transfer regions without spacer grid effects. For the enhancement heat transfer region in consequence of the spacer grid, all the existing models underestimate the heat transfer abilities at supercritical condition. In addition, the enhancement factor of spacer grid design and flow conditions were evaluated. Based on these enhancement factors, a new heat transfer model for space grid effect was developed and the accuracy of heat transfer in the downstream of spacer grid was significantly improved.

## 1. Introduction

As the only Water-Cooled-Reactor in Generation IV reactors (Gen-IV) [1], research activities on Supercritical Water-cooled Reactor (SCWR) are ongoing worldwide due to the system simplification and higher thermal efficiency. The technical extension from supercritical fossil power plants is another advantage to SCWR because the Supercritical Fluids (SCFs) have been widely applied in energy engineering for several decades. In the GEN-IV nuclear energy systems, supercritical water and $CO_2$ have been considered as promising coolants in the nuclear reactor or as working fluids in the power conversion system. Therefore, the knowledge of heat transfer to SCFs is required for the design and for the safe operation of nuclear reactors and other heat transport systems. Even though the research efforts on thermal hydraulic characteristics of supercritical fluids stated in 1930s [2], the accrued prediction of heat transfer to SCFs still remains a challenging issue, because of the deficiency in the mechanistic understanding. The dramatic change of fluid properties causes the unusual flow and heat transfer phenomenon compared with convective flow at subcritical condition. Due to the complexity of the physical properties change, an accurate prediction of heat transfer at supercritical condition is quite hard to accomplish, especially near pseudo-critical point. In engineering field of SCWR design, one of the possibility is to use the empirical heat transfer models to predict the heat transfer coefficient (HTC) at supercritical condition. In the past 20 years, experiments of heat transfer of circular tube at supercritical pressure were reported and many heat transfer correlations based on the experiment were proved effective in heat transfer at supercritical condition. These works are well reviewed by Pioro et al. [3,4], Cheng et al. [5] and Huang et al. [6]. Among these reference publications provided by reviewers, most of them are focused on convective heat transfer experiments above critical point with water, Freon and $CO_2$ flowing inside a heated circular tube.

In the future SCWR design, none-circular geometries such as rod bundles are widely used. However, heat transfer phenomenon in rod bundles are quite different from circular tube because of the none-circular geometry and flow mixing by spacers. With the implementation of spacers, thermal boundary layer of fluid downstream is destroyed and heat transfer is significantly improved due to such 'spacer effect'. However, the effect of spacer makes it even more complex to investigate the heat transfer phenomenon in rod bundle geometries. It is well agreed by the community [7,8] that at a certain flow parameter combination, the so-called heat trans-

* Corresponding author.
*E-mail addresses:* meng.zhao@kit.edu (M. Zhao), fangnian.wang@kit.edu (F. Wang), aurelian.badea@kit.edu (A.F. Badea).

**Nomenclature**

| | | |
|---|---|---|
| A | Enhancement coefficient of spacer grid | - |
| B | Decay coefficient of spacer grid | - |
| Bu | Buoyancy number, $Bu = \frac{\overline{Gr}}{\mathrm{Re}^{2.7}\overline{\mathrm{Pr}}^{0.5}}$ | - |
| Cp | specific heat | J/(kg.K) |
| $\overline{Cp}$ | Average specific heat, $\overline{Cp} = \frac{h_w - h_b}{T_w - T_b}$ | J/(kg.K) |
| D | Diameter | m |
| $D_h$ | Hydraulic diameter | m |
| F | Correction factor | - |
| G | Mass flow rate | kg/(m$^2$.s ) |
| Gr | Grashof number | - |
| $\overline{Gr}$ | Average Grashof number, $\overline{Gr} = \frac{\rho_b(\rho_b - \overline{\rho})gD^3}{{\mu_b}^2}$ | - |
| h | specific enthalpy | J/kg |
| HTC | Heat transfer coefficient | W/(m$^2$.K) |
| I | DC current | A |
| L | Length | m |
| N | Data number | - |
| Nu | Nusselt number | |
| Nu ratio | Local Nu number to Nu number without spacer effect $Nu\ ratio = \frac{Nu_b}{Nu_\infty}$ | - |
| P/D | Pitch to diameter ratio | - |
| Pr | Prandtl number | - |
| $\overline{\mathrm{Pr}}$ | Average Prandtl number, $\overline{\mathrm{Pr}} = \frac{\mu\overline{Cp}}{\lambda}$ | - |
| q | Heat flux | W/m$^2$ |
| Re | Reynolds number | - |
| T , t | Temperature | K, °C |
| U | DC voltage | V |
| x | Distance to the spacer grid | m |

*Greek letters*

| | | |
|---|---|---|
| $\beta$ | Thermal expansion coefficient | K$^{-1}$ |
| $\sigma$ | Standard deviation | - |
| $\varepsilon$ | Blockage ratio of spacer grid | - |
| $\eta$ | Thermal efficiency | - |
| $\lambda$ | Thermal conductivity | W/(m.K) |
| $\mu$ | Dynamic viscosity | kg/(m.s) Mean deviation - |
| $\pi_A$ | Acceleration number, $\pi_A = \frac{\beta q}{CpG}$ | - |
| $\rho$ | Density | kg/m$^3$ |
| $\overline{\rho}$ | Average Density, $\overline{\rho} = \frac{1}{T_w - T_b}\int_{T_b}^{T_W} \rho dT$ | kg/m$^3$ |

*Subscripts*

| | |
|---|---|
| $\infty$ | "Infinity distance", in this investigation refers to Nu without spacer effect |
| b | Bulk fluid |
| in | inside |
| out | outside |
| PC | pseudo-critical |
| v | volume |
| w | wall |

fer deterioration (HTD) occurs with dramatic temperature increase of heated tube. In the supercritical energy system design, the engineers must avoid the HTD and keep the fuel cladding temperature below the allowable limit. It must be pointed out that the present empirical correlation for predicting HTD region is mainly based on circular tube experiment and whether HTD occurs or not in rod bundle geometries is still controversial. Some research groups (e.g. Kirillov et al. [9] and Razumovskiy et al. [10,11]) reported the deterioration of rod bundle experimentally, while other researchers (e.g. Mori et al. [12]) believed that the thermal boundary layer was encountered in rod bundles because of the spacer mixing, so that no heat transfer deterioration should occur in rod bundles.

Up to now, the literatures of heat transfer experiment in rod bundles at supercritical condition are still limited. Before 1990's, most of the open literatures were carried out by the former Soviet Union researchers and institutes. Dyadyakin et al. [13] conducted experiments with a tight-lattice 7-rod bundles and clearly observed the significant pressure oscillations at the condition of high mass fluxes and high heat fluxes. They also proposed a correlation about HTC in rod bundles. Silin et al. [14] carried out a large number of the experiments of supercritical water flowing inside large-rod bundles based on the background of Russian Pressurized Water Reactor (PWR) operating at supercritical condition. However, his research group did not find the heat transfer deterioration after operating the numerous experiments at the conditions which heat transfer deterioration occurred in tubes.

In recent 5 years, some experiment of heat transfer in rod bundles were reported in China. To investigate the 2 × 2 rod bundles with spacer grid and spacer wire, Wang et al. [15,16] and his research group from Xi'an Jiao Tong University designed an experiment test section to measure the heat transfer coefficient of supercritical water in 2 × 2 rod bundles. The rod bundles were heated by electric power and 1.2mm wire-wrap spacer with 200mm axial pitch were used to keep the position of rods. The HTC and the circumferential heat transfer difference were discussed and experiment databank were obtained to support the SCWR design [17].

In the frame of the international collaboration project Supercritical Water Reactor Fuel Qualification Test (SCWR-FQT) [18], experiment of 2 × 2 rod bundles with spacer grid and spacer wire [19,20] were performed by SWAMUP facility in Shanghai Jiao Tong University to make significant progress towards the design, analysis and licensing of the Fuel Qualification Test facility cooled with supercritical water in the research reactor LVR-15 [21]. The experiment test sections contain 4 fuel rods with two different rod diameters (8 mm rod diameter in spacer grid, 10mm rod diameter in spacer wire, P/D various from 1.18 to 1.3). Similar to the High Performance Light Water Reactor (HPLWR) assembly concept [22], the heated rods were arranged inside a square assembly box and the fluid flows through the gaps between the rods and square box.

Table 1 gives a detail review of the heat transfer experiments of supercritical water in rod bundle geometries. From all the references [16,19] of rod bundles with spacer grid, the local effect of spacer grid is significantly strong and heat transfer is obviously enhanced near spacer grid. In SCWR, the spacer grid in rod bundle is an indispensable part in the fuel rod assembly. It is widely used to accurate position of fuel bundles, to determinate the relative position between the fuel bundles, and to optimize the fluid motion through the vibration of fuel components. The spacer grid blocks part of the cross-section so that the fluid disturbance in the subchannel is strengthened. On the other hand, the thermal boundary layer can be destroyed by the turbulence in the downstream of the spacer grid and the heat transfer beneath the thermal boundary layers switches from thermal conduction to forced convection. Due to these two factors, the heat transfer downstream the spacer is significantly enhanced. Song et al. [23] and Xiao et al. [24] founded that the highest heat transfer augmentation occurred downstream the spacer grid and the enhancement decreased with the increasing distance from the spacer.

Strictly speaking, the investigations of HT in rod bundles at a cross-section can be only done in 'bare rod' to separate the spacer effect. In the investigations of Silin et al. [14], Wang et al. [15] and Gu et al. [19], experiments to study the heat transfer to supercritical water in bare rod bundles were carried out with few experiment data. In their investigations, a non-uniform distribution of wall temperature was clearly observed on the circumference direction of the rods. However, it is unfortunately that both the experiments of Silin et al. [14] and Gu et al. [19] are designed to be quite short (about 600-800mm) to prevent rod blending, so that exper-

**Table 1**
List of supercritical water heat transfer experiment in rod bundles.

| Author | Background | Year | Fluid | Geometry | Parameter |
|---|---|---|---|---|---|
| Dyadyakin [13] | LWR in SCW | 1977 | $H_2O$ | 7 Rod Bundles | P=24.5MPa<br>G=500-4000kg/m$^2$/s<br>q up to 4.7MW/m$^2$ |
| Silin [14] | LWR in SCW<br>(B-500-SKDI) | 1993 | $H_2O$ | Rod Bundles in<br>Fuel Assembles | P=23.5-29.4MPa<br>G=500-4000kg/m$^2$/s<br>q=0.18-4.5MW/m$^2$ |
| Razumovskiy [10,11] | SCWR | 2008<br>2009 | $H_2O$ | 7 Rod Bundles<br>3 Rod Bundles | P=22.6-27.5MPa<br>G=700-2700kg/m$^2$/s<br>q=0.5-4.58MW/m$^2$ |
| Gu [19,20] | SCWR-M | 2013 | $H_2O$ | 4 Rod Bundles | P=23-26Mpa<br>G=450-1500kg/m$^2$/s<br>Q=0.4-1.5MW/m$^2$ |
| Wang [15,16] | SCWR | 2014 | $H_2O$ | 4 Rod Bundles | P=23-28MPa<br>G=350-1000kg/m$^2$/s<br>q=0.2-1.0MW/m$^2$ |

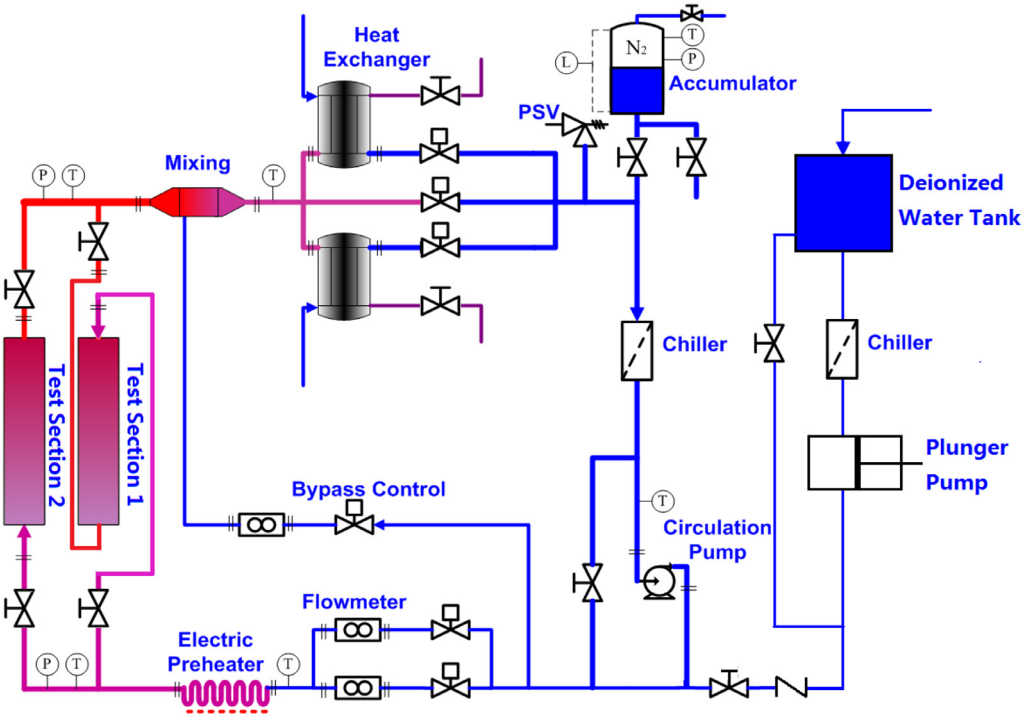


**Fig. 1.** Schematic of the SWAMUP test facility [25].

iment data without inlet effect are quite few to develop the new heat transfer models.

This paper carried out a large number of experiment in 2 × 2 rod bundles with spacer grid and the quality of experiment data was analyzed. With the databank obtained by the experiment, further work has been done by separating the experiment points into two parts: (1) data points far away from the spacer grid (fully-developed region without spacer effect) and (2) data points near spacer grid (within range of the spacer effect). Several correlations developed in circular tube were evaluated with rod bundle data without spacer effect and new heat transfer model on the decay behavior by spacer grids was developed.

## 2. Experiment work and databank of heat transfer

The experiment of heat transfer of supercritical water flowing in 2 × 2 rod bundles were carried out at the SWAMUP test facility [25], shown in Fig. 1. The test facility is a closed circulation loop and consists of a main test loop, a cooling water loop, a water purification loop, and a high speed data acquisition system by National Instruments. The test loop is constructed for system pressure up to 30 MPa, fluid temperature up to 550°C, mass flow rate up to 1.3 kg/s and electrical heated power up to 1.2 MW. Supercritical water flows vertically through the test sections and flow directions can be set to upward or downward.

The test section, as shown in Fig. 2, is consisted in four Inconel heated tubes (with 8 mm outer diameter and 1.5 mm thickness) and ceramic square tubes (one set with 20.32×20.32mm and another set with 23.2 ×23.2mm ), forming hydraulic diameters of 4.6mm and 7.6mm. The length of the channel is 1328 mm and is averagely separated by 5 to 6 space grids. The four heated tubes are installed with a sliding thermal couple system to measure the inner sidewall temperature. The outer square tube is unheated and covered with fiberglass insulation to minimize heating loss. The design of test sections as well as sliding thermal couple system is shown in Fig. 2 and 3. The experimental procedure measured DC voltage, current, pressure, mass flux, fluid temperature, tube inner wall temperature, thermal efficiency and the axial height. The detailed uncertainties of measurement parameters were shown in Table 2.

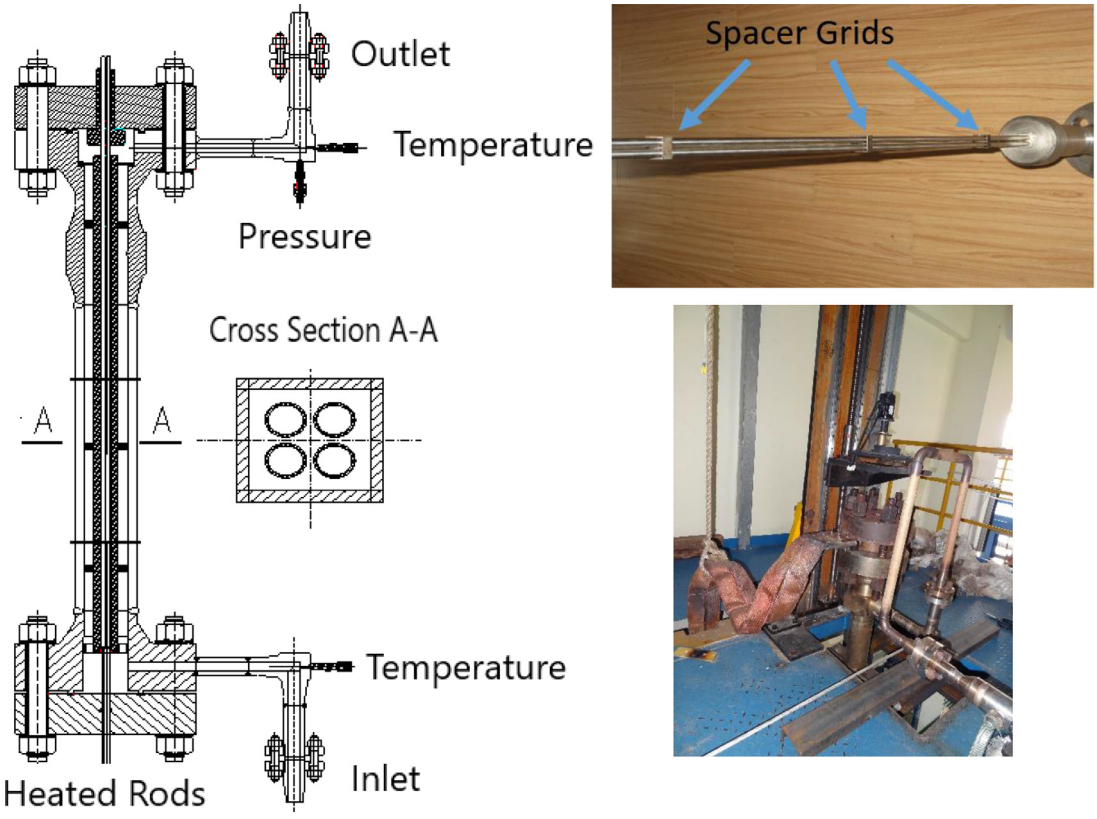


**Fig. 2.** Schematic diagram of test section (left), heated rod (upper right) and sliding thermal couple system (lower right).

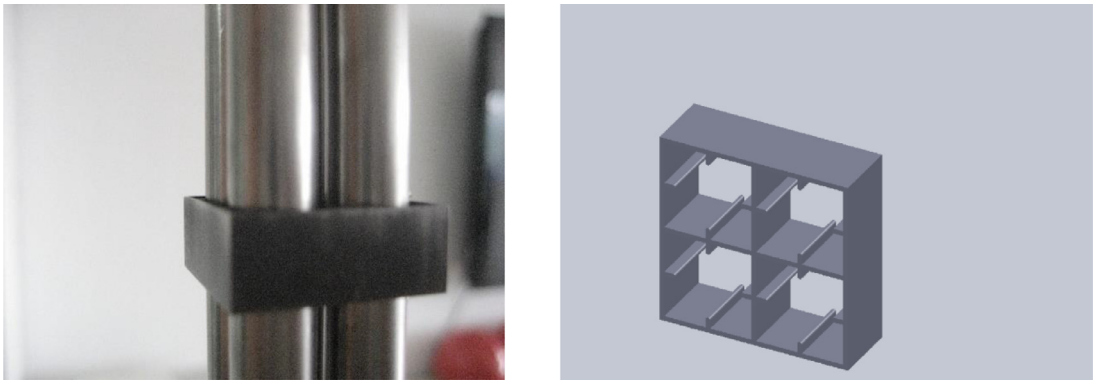

**Fig. 3.** The spacer grid in the test section of 2 × 2 rod bundles.

**Table 2**
Uncertainties of primary parameters.

| Parameters | Maximum uncertainty |
|---|---|
| Pressure | ±0.2 % |
| Mass flow rate | ±0.4 % |
| Temperature | ±1.5 °C |
| DC current | ±1.0 % |
| DC voltage | ±1.0 % |
| Heated tube diameter | ±0.04 mm |
| Heated tube thickness | ±0.02 mm |
| None-heated tube diameter | ±0.10 mm |
| TC axial measurement position | ±0.05 mm |

Fig. 3 shows the spacer grid in the test section of 2 × 2 rod bundles. The grid spacer manufactured from 304 stainless steel was installed in the axial direction of the rod bundle. The spacer grid was designed as simple geometry without mixing vane. To ensure the data points with spacer effect and in full developed zone, 5 or 6 spacers were equidistantly installed in the axial direction.

Fig. 4 shows the measurement positions of wall temperature by the thermal couple system. Wall temperatures at the inner side of heated tube were measured by sliding thermocouples. Because the calculation of heat transfer coefficient must use the tube outside temperature, the outer surface temperature is calculated with the following formula.

$$T_{w-out} = T_{w-in} + \frac{q_v}{4\lambda_w}\left[\left(\frac{D_{out}}{2}\right)^2 - \left(\frac{D_{in}}{2}\right)^2\right] - \frac{q_v}{2\lambda_w}\left(\frac{D_{out}}{2}\right)^2 \ln\left(\frac{D_{in}}{D_{out}}\right) \quad (1)$$

$$q_v = \frac{4U \cdot I}{\pi\left({D_{out}}^2 - {D_{in}}^2\right)L}\eta \quad (2)$$

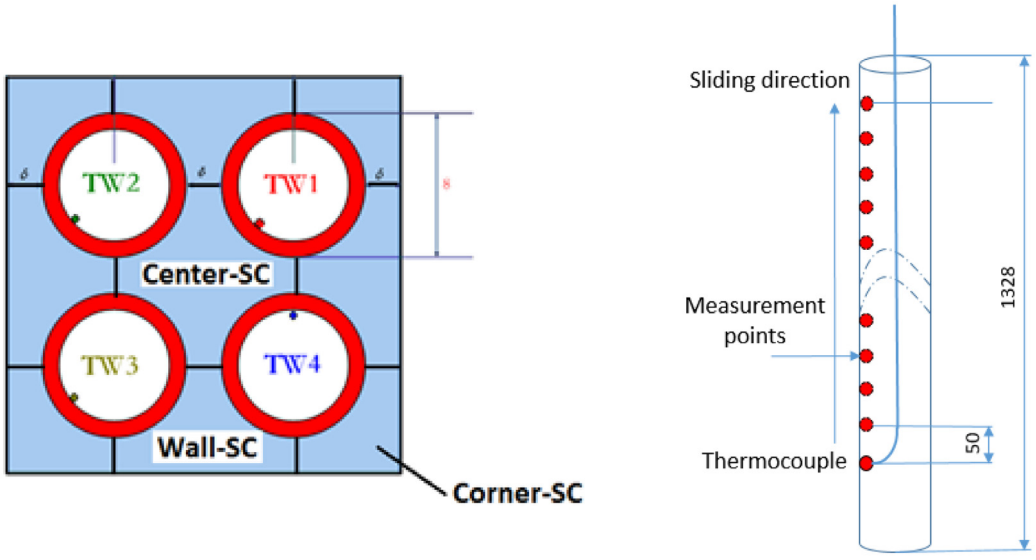


**Fig. 4.** Sliding Thermal-couples and measurement points in the test section (unit: mm).

**Table 3**
The geometries of sub-channels.

| Test sections | Sub-channels | Number | Flow area/mm$^2$ | Blockage area/mm$^2$ | Blockage ratio/- |
|---|---|---|---|---|---|
| A with P/D=1.18 | Center | 1 | 38.85 | 10.02 | 0.258 |
| | Wall | 4 | 26.22 | 7.55 | 0.288 |
| | Corner | 4 | 17.03 | 5.18 | 0.304 |
| | Cross-section average | - | 211.85 | 61.65 | 0.291 |
| B with P/D=1.3 | Center | 1 | 57.91 | 14.07 | 0.243 |
| | Wall | 4 | 41.44 | 11.15 | 0.269 |
| | Corner | 4 | 28.38 | 8.32 | 0.293 |
| | Cross-section average | - | 337.18 | 93.06 | 0.276 |

**Table 4**
Parameter ranges for SCW HT in rod-bundles with spacer grid.

| Parameter range | | | | Number of data |
|---|---|---|---|---|
| Hydraulic diameter (mm) | Pressure (MPa) | Mass flux (kg/m$^2$/s) | Heat flux (MW/m$^2$) | |
| 4.66 and 7.60 | 22.8 – 26.2 | 460 - 1750 | 0.45 - 1.5 | 5674 |

The 4 sliding thermal couples can move axially and circumferentially. In the experiment, each sliding thermal couple moves up and down to measure 20-25 points in axial position. To investigate the heat transfer in different sub-channels, the circumferential positions of thermal couples were arranged to the direction of test section center (as shown in TW1 of Fig. 4 left), the direction of none heated wall (as shown in TW2), the direction of corner (as shown in TW3) and rod gap (as shown in TW4). The detail geometries of flow sub-channels and blockage ratio of spacer grid in each test section are shown in Table 3.

Table 4 shows the experimental data of heat transfer of supercritical water flowing in 2 × 2 rod with spacer grid. Considering the typical condition in SCWR applications, the experiments were carried out in steady state with the following parameter range: pressure various from 22.8 to 26.2 MPa, mass flux 460 to 1750 kg/m$^2$/s (with Re number from 3 × $10^4$ to 1.8 × $10^5$) and heat flux up to 1.5MW/m$^2$. According to Yamagata's proposal [8] about heat transfer deterioration, about 45% of data points are above the Yamagata line of q (kW/m$^2$) =0.2G$^{1.2}$ ($kg/m^2/s$), so that the phenomenon of heat transfer deterioration (HTD), at least strong heat transfer reduction, might occur. In order to predict HTC at cases with strong heat transfer reduction or HTD, test data for the developing the new correlation should achieve high quality and reliability by the following aspects:

(a) **Consideration of thermal energy balance**

The databank of 2 × 2 rod bundles with spacer grid provided fluid inlet and outlet temperature, bulk temperature at cross-section, heat flux and mass flux from the measurement. The enthalpy rises between the inlet or outlet and local parameters are compared with the enthalpy rise using the energy balance, i.e. from the heating power and mass flux. When the deviation between both enthalpy rises is larger than 10%, the test point will be removed from the databank. In this way, 115 data points were excluded from the total number of 5674.

(a) **Consideration of reproducibility**

Reproducibility has been recognized as one of the main issues affecting the reliability of the test data. The deviation between the experimental data may occur, even though the experiment data at the same conditions. The difference between the test data is usually explained with the experimental uncertainties. An own developed procedure was used to assess the intrinsic consistency of the experimental information (values of the Nusselt number at bulk fluid,$Nu_b$) contained in the databank. The detail reproducibility

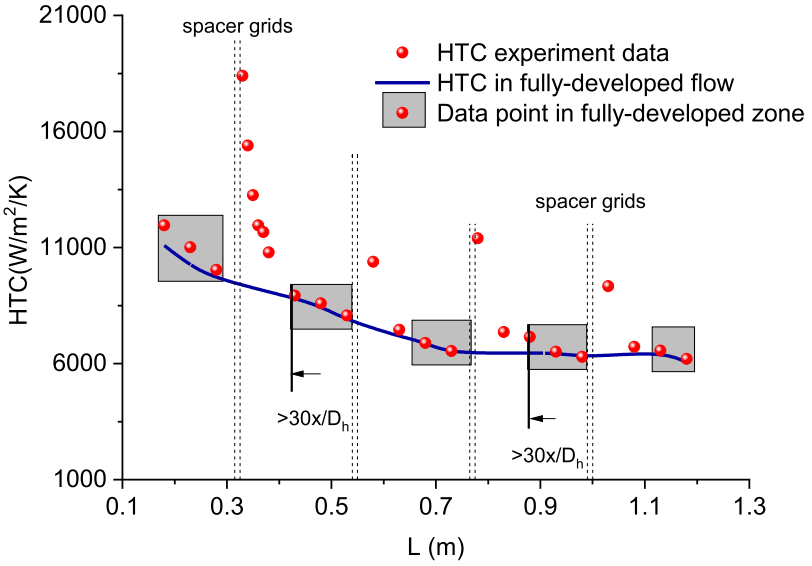


**Fig. 5.** HTC versus axial position with spacer effect.

**Table 5**
Quality assessment of the original databank.

| | Data points | Remarks |
|---|---|---|
| Original Databank | 5674 | Including 115 points of energy balance difference and 826 points of bad reproducibility |
| Full databank | 3691 | Data quality was proved by the considerations of (a) and (b) |
| Restricted databank | 1042 | Data without neighbouring points |

method can be found in another paper of the author [26] (See formula 6-11 of reference [26]). After the reproducibility check, only 4733 data points remain and 826 data points were excluded due to the bad reproducibility. Furthermore, there are 1042 data points don't have neighbouring data points. Finally, the remain data (3691 points) were defined as full databank. Due to their reproducibility cannot be proven, 1042 data points were defied as restricted databank. In the present study, only the full databank (3691 points) were taken for the development of the new correlations. However, in the correlation assessment, both full data (3691 points) and restricted data (1042 points) can be used. Table 5 shows the summary of quality assessment of the original databank.

## 3. Heat transfer of none-spacer-effect

### 3.1. Fully-developed regions

Fig. 5 shows the heat transfer coefficient between heated tube and fluid versus the axial position. The HTC were obtained by the average outer tube wall temperature of TW1-TW3 (as shown in Fig. 4 left), neglecting the circumferential wall temperature difference. At the position downstream of the spacer, heat transfer is strongly enhanced because the fluid flows through the spacer grid. It is clear that the maximum enhancement point is just downstream of the spacer grid, or spacer outlet. With the axial distance far from the spacer outlet, this enhancement phenomenon decays significantly. When the distance reaches 30 times of $x/D_h$ of the spacer, the influence of spacer grids almost disappears and heat transfer from 30 times of $x/D_h$ can be considered as bare rod. Thus, such heat transfer enhancement due to the spacer effect within a certain range and position of $x/D_h$ >30 can be considered as none-spacer-effect region, or fully-developed region. Table 6 shows the numbers of data points in fully-developed zone and spacer grid influenced zone. In full databank, about 1500 data points are located in fully-developed region and more than 2200 data points can be used to investigate the spacer effect.

### 3.2. Comparison with heat transfer correlations

Turbulent flow and convective heat transfer in rod bundle geometries differ from that in circular tube geometries. Since the correlations developed for rod bundles are limited. It is an option to compare the existing tube-correlation of supercritical fluid to the rod bundles data. In the open literature, several correlations were used to predict the HTC at rod bundles or other none-circular geometries [13,27]. The Dittus-Boelter correlation [28] is the earliest and the most common correlation to predict HTCs in circular tubes and many correlations after are modified with fluid properties from Dittus-Boelter correlation. Correlations of Bishop [27] and Swenson [29], which were developed by their own experiment of supercritical water, are also frequently used in predict HTC. Watts-Chou [30] correlation is from the experimentally studied of the mix convection heat transfer to supercritical water and the buoyancy effects were taken into consideration when deriving the modified factor. Moreover, Cheng [31] proposed a correlation for the prediction of heat transfer to supercritical water based on the acceleration parameter $\pi_A$. Cheng's correlation was proved with high accuracy by large number of databank of circular tube. The correlation of Jackson and the correlation of Bae were developed in $CO_2$ by the experiment. These two correlations are based on the Buoyancy number Bu and the effect of buoyancy to heat transfer in $CO_2$, which is similar to water. In this study, Dittus-Boelter correlation, Bishop Correlation, Swenson Correlations, Jackson [32] Correlation, Watts- Chou Correlation, Cheng correlation, Kirillov Correlation [33] and Bae correlation [34] were selected to compare with experiment data without spacer effect. The detail structure of correlations are shown in Table 7.

These 8 correlations were applied in comparison with rod bundle databank (the combination of the full and the restricted databank) without spacer effect. It is noted that the Bae correlation [34] listed in Table 7 was developed by their tube and annuli experiment of carbon dioxide with the range of dimensionless number Bu from $5 \times 10^{-8}$ to $1 \times 10^{-4}$ with 5 piecewise functions. For the case of $Bu < 10^{-8}$ and $Bu > 10^{-4}$, the function of Bu number

**Table 6**
Data points with spacer effect and in fully-developed region.

| Databank types | Total number | Data with spacer effect | Data in fully-developed region |
|---|---|---|---|
| Full databank | 3691 | 2215 | 1476 |
| Restricted databank | 1042 | 681 | 361 |

**Table 7**
Frequently used correlations in heat transfer of supercritical water and $CO_2$.

| Authors | Correlations |
|---|---|
| Dittus-Boelter [28] | $Nu_b = 0.023 Re_b^{0.8} Pr_b^{0.33}$ |
| Bishop [27] | $Nu_b = 0.0069 Re_b^{0.9} \overline{Pr}_b^{0.66} (\frac{\rho_w}{\rho_b})^{0.43} (1 + 2.4\frac{D}{x})$ |
| Swenson [29] | $Nu_w = 0.00459 Re_w^{0.923} \overline{Pr}_w^{0.613} (\frac{\rho_w}{\rho_b})^{0.231}$ |
| Jackson [32] | $Nu_b = 0.0183 Re_b^{0.82} Pr_b^{0.5} (\frac{\rho_w}{\rho_b})^{0.3} (\frac{\overline{Cp}}{Cp_b})^n$ |
| | $n = 0.4 \quad if\ T_b < T_w < T_{pc}\ or\ 1.2T_{pc} < T_b < T_w$ |
| | $n = 0.4 + 0.2(\frac{T_w}{T_{pc}} - 1) \quad if\ T_b < T_{pc} < T_w$ |
| | $n = 0.4 + 0.2(\frac{T_w}{T_{pc}} - 1)[1 - 5(\frac{T_b}{T_{pc}} - 1)] \quad if\ T_b < T_w\ and\ T_{pc} < T_b < 1.2T_{pc}$ |
| Cheng [31] | $Nu_b = 0.023 Re_b^{0.8} Pr_b^{0.33} F$ |
| | $F = min(F_1, F_2)$ |
| | $F_1 = 0.85 + 0.776\ (\pi_A \cdot 10^3)^{2.4}$ |
| | $F_2 = \frac{0.48}{(\pi_{A,PC} \cdot 10^3)^{1.55}} + 1.21 \cdot (1 - \frac{\pi_A}{\pi_{A,PC}})$ |
| | $Nu_b = 0.021 Re_b^{0.8} \overline{Pr}_b^{0.55} (\frac{\rho_w}{\rho_b})^{0.35} f(Bu)$ |
| Watts-Chou [30] | $f(Bu) = 1 \quad if\ \ Bu \le 10^{-5}$ |
| | $f(Bu) = (1 - Bu)^{0.295} \quad if\ \ 10^{-5} < Bu \le 10^{-4}$ |
| | $f(Bu) = (7000Bu)^{0.295} \quad if\ \ Bu > 10^{-4}$ |
| Kirillov [33] | $Nu_0 = 0.023 Re^{0.8} \overline{Pr}^{0.4} C_t$ |
| | $C_t = (\mu_b/\mu_w)^n$ |
| | $n = \begin{cases} 0.11 & heating \\ 0.25 & cooling \end{cases}$ |
| | $Nu = \begin{cases} Nu_0 (\frac{\overline{c_p}}{c_{pb}})^n (\frac{\rho_w}{\rho_b})^m & k^* < 0.01 \\ Nu_0 (\frac{\overline{c_p}}{c_{pb}})^n (\frac{\rho_w}{\rho_b})^m \varphi(k^*) & k^* > 0.01 \end{cases}$ |
| | $k^* = (1 - \frac{\rho_w}{\rho_b}) \frac{Gr}{Re^2}$ |
| | $n = \begin{cases} 0.7 & (\overline{c_p}/c_{pb}) \ge 1\ vertical\ upward\ flow \\ other\ conditions & \begin{cases} 0.4 & (t_w/t_{pc}) < 1\ and\ (\overline{t_b}/t_{pc}) > 1.2 \\ 0.22 + 0.18(t_w/t_{pc}) & (t_w/t_{pc}) > 1\ and\ (\overline{t_b}/t_{pc}) < 1 \\ 0.9(\overline{t_b}/t_{pc})(1 - t_w/t_{pc}) + 1.08(t_w/t_{pc}) - 0.68 & (t_w/t_{pc}) > 1\ and\ 1 < (\overline{t_b}/t_{pc}) < 1.2 \end{cases} \end{cases}$ |
| | $m = \begin{cases} 0.4 & vertical\ upward\ flow \\ 0.3 & vertical\ downward\ and\ horizontal\ flow \end{cases}$ |
| | $\varphi(k^*) = \begin{cases} 0.79782686 - 1.6459037 \ln k^* - 2.7547316 (\ln k^*)^2 - 1.7422714 (\ln k^*)^3 \\ -0.54805506 (\ln k^*)^4 - 0.086914323 (\ln k^*)^5 - 0.0055187343 (\ln k^*)^6 \quad k^* \le 0.4 \\ 1.4 (k^*)^{0.37} \quad k^* > 0.4 \end{cases}$ |
| Bae [34] | $Nu_b = 0.021 Re_b^{0.82} Pr_b^{0.5} (\frac{\rho_w}{\rho_b})^{0.3} (\frac{\overline{Cp}}{Cp_b})^n$ |
| | $n = 0.4 \quad if\ T_b < T_w < T_{pc}\ or\ 1.2T_{pc} < T_b < T_w$ |
| | $n = 0.4 + 0.2(\frac{T_w}{T_{pc}} - 1) \quad if\ T_b < T_{pc} < T_w$ |
| | $n = 0.4 + 0.2(\frac{T_w}{T_{pc}} - 1)[1 - 5(\frac{T_b}{T_{pc}} - 1)] \quad if\ T_b < T_w\ and\ T_{pc} < T_b < 1.2T_{pc}$ |
| | $f(Bu) = (1 + 1.0 \times 10^8 Bu)^{-0.032} \quad 5 \times 10^{-8} < Bu < 7 \times 10^{-7}$ |
| | $f(Bu) = 0.0185 Bu^{-0.43465} \quad 7 \times 10^{-7} < Bu < 1 \times 10^{-6}$ |
| | $f(Bu) = 0.75 \quad 1 \times 10^{-6} < Bu < 1 \times 10^{-5}$ |
| | $f(Bu) = 0.0119 Bu^{-0.36} \quad 1 \times 10^{-5} < Bu < 3 \times 10^{-5}$ |
| | $f(Bu) = 32.4 Bu^{0.40} \quad 3 \times 10^{-5} < Bu < 1 \times 10^{-4}$ |

still uses first formula 12(a) and the last formula 12(e) of reference [34] by extending the scope of application to fit for all the conditions. Fig. 6 shows the predicted Nu number against the experimental data. The Nu number was calculated from the correlations and the fluid properties were calculated from the NIST [35].

It can be seen from Fig. 6(a), the Nu predicted by Dittus-Boelter correlation is significantly higher than the Nu from experimental data and the scattering is observed in all the test data with different mass flow rates. In Fig. 6(c) and 6(f), the Nu numbers predicted by Swenson and Kirillov correlations are higher than that from experiment data, especially at the condition of high mass flow rate.

Shown from Fig. 6(b), 6(d) and 6(e), most of the data points are within ±25% of Nu number ratio. In addition, for Cheng and Watts-Chou correlation, a good agreement between correlation prediction and experiment data can be seen at lower mass flow rate. With the increase of mass flow rate, the Nu number increases significantly because it is generally believed that Nu is proportional to Re with a certain power level (in Dittus-Boelter correlation, the power level is 0.8 and most of the correlation is developed from Dittus-Boelter correlation and has the similar structure). However, at the high mass flow rate, e.g. mass flow rate = 1500 and 1800 kg/m$^2$/s, the scattering of these three correlations increases slightly and parts of the data are out of ±25% of Nu number ratio.

For the correlations developed from $CO_2$ and considered the buoyancy of fluid, the accuracy of Jackson and Bae correlations, shown in Fig. 6(g) and 6(h) is slightly lower than that developed from water. For the lower mass flux or lower Re number, Bae correlation can predict the Nu exactly due to the contributions of piecewise functions at high Bu number.

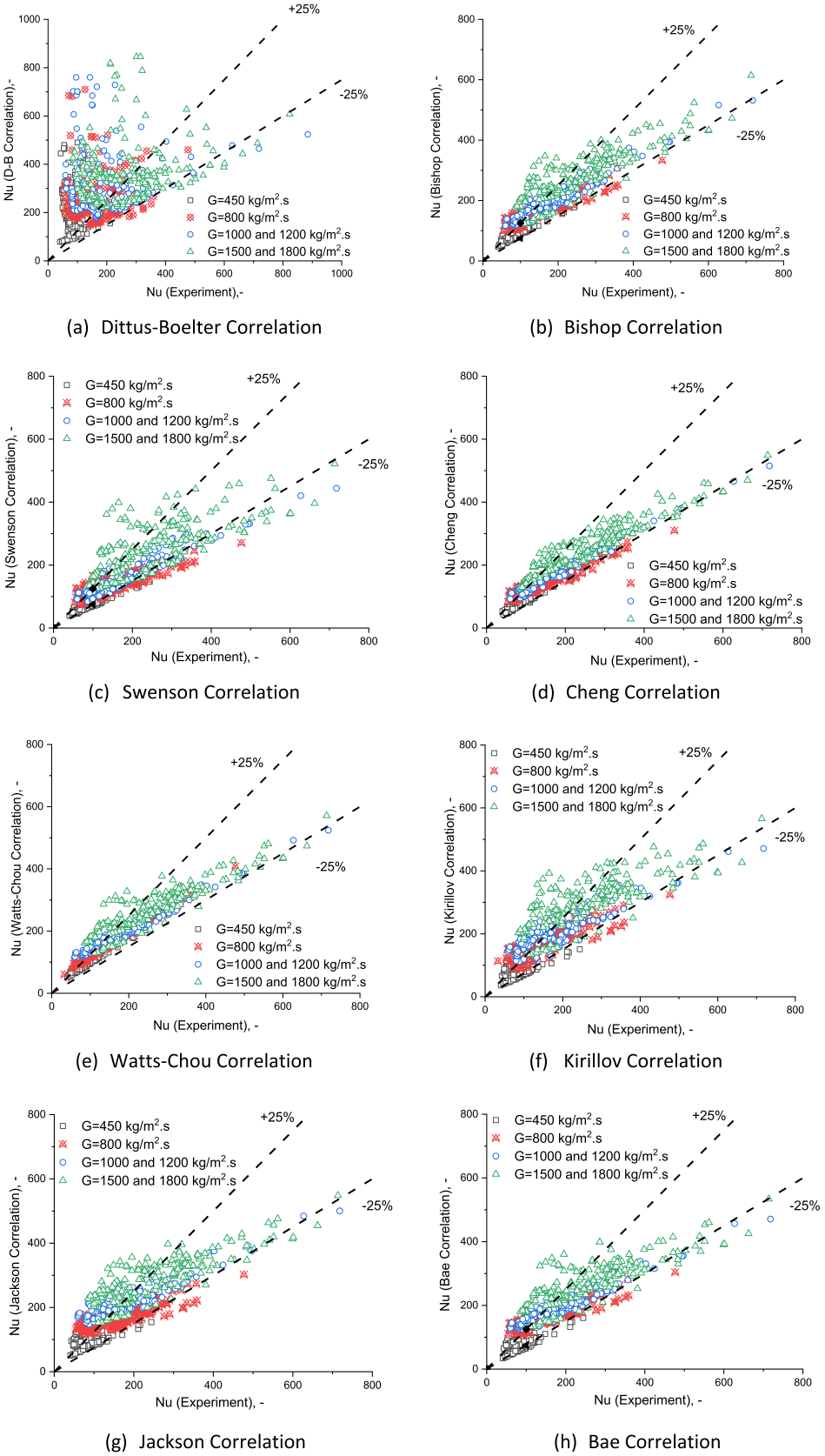


**Fig. 6.** The comparison Nu between the predictions by correlations and the experimental data.

**Table 8**
Correlation accuracy against database for 2 × 2 rod bundles in fully-developed region.

| Correlations | $\mu$ (%) | $\sigma$ (%) | Percentage of databank within the band of | | | | |
|---|---|---|---|---|---|---|---|
| | | | ±10% | ±20% | ±30% | ±40% | ±50% |
| Dittus-Boelter | 54.1 | 51.8 | 13.3 | 26.1 | 35.0 | 53.5 | 67.2 |
| Bishop | 13.0 | 20.1 | 38.6 | 64.8 | 78.0 | 93.8 | 98.5 |
| Swenson | 29.9 | 33.6 | 30.2 | 65.6 | 86.3 | 96.1 | 98.5 |
| Jackson | 26.0 | 34.4 | 25.0 | 43.5 | 57.5 | 83.7 | 94.2 |
| Cheng | 7.4 | 21.5 | 37.2 | 59.1 | 74.2 | 85.2 | 96.6 |
| Watts-Chou | 12.5 | 18.6 | 62.5 | 83.6 | 91.8 | 99.2 | 99.5 |
| Kirillov | 22.1 | 36.1 | 22.6 | 43.9 | 62.6 | 87.8 | 96.5 |
| Bae | 25.0 | 26.8 | 50.1 | 80.2 | 88.0 | 98.5 | 99.6 |

To achieve quantitative assessment, the mean deviation μ, defined in formula (4), and standard deviation $\sigma$, defined in formula (5), were calculated for data points of full and restricted databank.

$$\mu_i = \frac{Nu(correlation)_i - Nu(Experiment)_i}{Nu(Experiment)_i} \times 100\% \tag{3}$$

$$\mu = \frac{1}{N}\sum_{i=1}^{N}\mu_i \tag{4}$$

$$\sigma = \sqrt{\frac{1}{N-1}\sum_{i=1}^{N}(\mu_i - \mu)^2} \tag{5}$$

Table 8 shows the mean deviation μ, standard deviation $\sigma$ and the percentage of data predicted by correlation within an error band of ±10%, ±20%, ±30%, ±40%, and ±50%.

For the total 1837 data points in fully-developed zone (1476 test data points of full databank plus 361 test data points of restricted databank), large scatters between Dittus-Boelter correlation and experiment data were observed with more than 50% overestimate by the correlation. On the other hand, about 2/3 of data points of experiment were with 50% error band and only 13.3% of databank were within 10%. It is apparently that Dittus-Boelter correlation cannot be directly used with Nu or HTC prediction in rod bundle geometries. By comparing the accuracy of these 8 correlations, Bishop ($\mu = 13.0\%$), Cheng ($\mu = 7.4\%$) and Watts-Chou ($\mu = 12.5\%$) correlations show higher prediction accuracy with smaller mean deviation and standard deviation. From the perspective of mean deviation, Cheng correlations has the highest accuracy against the database in fully-developed region among the 8 selected correlations. However, it should be noted that the Cheng correlation has only 37.2% of data points in 10% error band and less than 3/4 data points were within 30% error band, even though the average scattering is the smallest. Therefore, the further investigation of cumulative data distribution, shown in Fig. 7, and probability data distribution, shown in Fig. 8, of the error parameter were carried out.

Fig. 7 shows the cumulative distribution curves of error parameter of the 8 correlations listed in Table 7 with the full and restricted test data. The figures confirm clearly the results in Table 8 and indicate that the correlation for Bishop, Cheng and Watts-Chou show better prediction than the other correlations. It is seen from Fig. 7(b) that for Watts-Chou correlation, very few test data have error parameter smaller than -0.2 and more than 80% of cumulate distribution locates at error parameter smaller than +0.2. In other word, the agreement between Watts-Chou correlation and experiment data is quite high within the ±20% error band and the slope near error parameter $\mu = 0$ is significantly higher than others. Comparison with Watts-Chou correlation, prediction accuracy of the Cheng correlations is slightly lower. This is because at the range of error parameter smaller than -0.2, there are already more than 20% of data and that means the correlation Cheng underestimates the Nu of some certain experiment cases. When the error

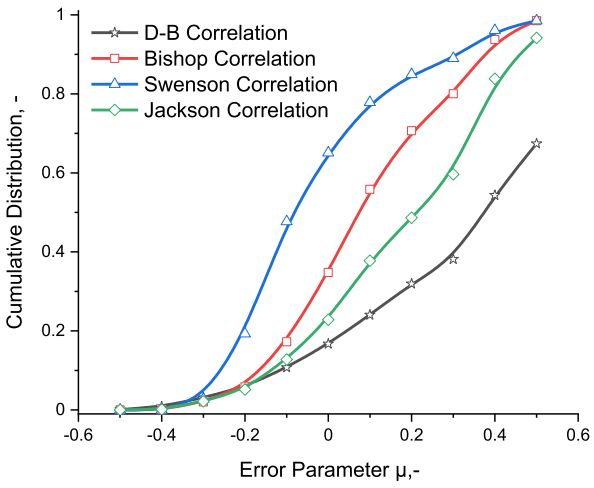


(a) Dittus-Boelter, Bishop, Swenson and Jackson Correlation

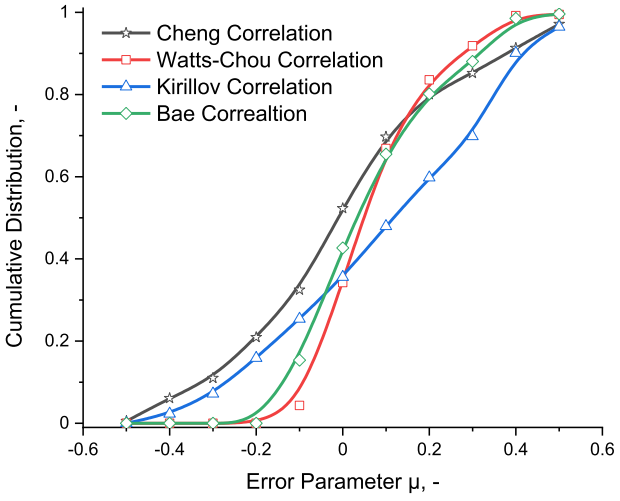


(b) Cheng, Watts-Chou, Kirillov and Bae Correlation

**Fig. 7.** Cumulative distribution of the error parameter.

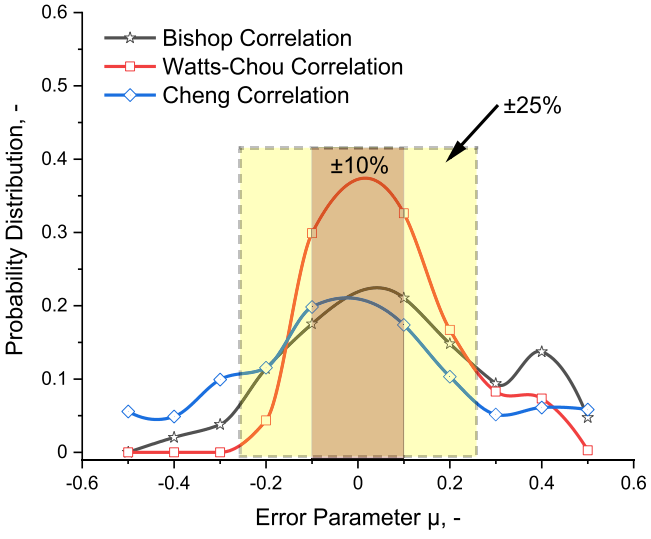


**Fig. 8.** Probability distribution of the error parameter.

parameter higher than +0.2, the slop of Cheng correlation is still high. It indicates that there are still considerable data points locate at error parameter larger than +0.2. For Cheng correlation, positive and negative deviations larger than ±20% cancel each other out so that Cheng correlation has the smallest mean deviation among the 8 correlations. This conclusion is confirmed again by the standard deviation of Cheng Correlation ($\sigma$=21.5%) is slightly larger than Watts-Chou ($\sigma$=18.6%) and Bishop Correlation ($\sigma$=20.1%).

Beside the deviation, another important criterion is error the band. It means that how many percentages of data points within the error range comparing with correlations. Fig. 8 illustrates the probability distribution of the error parameter from Bishop, Watts-Chou and Cheng Correlation. Comparing with the correlations of Bishop and Cheng, the probability distribution of the Watts-Chou correlation has a significant higher peak value. For Watts-Chou correlation, about 60% of probability distribution locates within ±10% error band and about 80% within ±20% error band. For Cheng Correlation and Bishop Correlation, there are a considerable probability distribution out of ±20% error band range. Considering both the deviation and the probability with high quantity in smaller error band, the Watts-Chou correlation can be used to predict the Nu of supercritical water flowing in rod bundles without spacer effect.

## 4. Heat transfer with spacer effect

### 4.1. Heat transfer enhancement in downstream of spacer grids

Spacer grids or spacer wires are important for the fuel assembly design in SCWR. They are used to keep a fixed distance between rods in a tight lattice to prevent damages of fuel assembly from flow induced vibration. Additionally, the spacer grids also bring a flow blockage and force the fluid flows in a higher local velocity. On the other hand, the destruction and redevelopment of boundary layers leads to a higher turbulent so that the heat transfer enhanced locally. Up to now, most of the investigations about the spacer effect are focused on subcritical cases, mainly based on PWR. In recent year, the importance of heat transfer enhancement in supercritical fluid due to the spacer effect has been widely recognized. In the design of SCWR, either spacer grid or spacer wire must be used. For spacer wire, the spacer effect is in the whole pitch or even in the total height. These investigations were well accomplished by Korean [36] and Chinese [37] researchers. Different from the spacer wire, spacer grid has a local augmentation effect and such enhancement in the downstream only will disappear slowly with the thermal boundary layers redevelop.

Kidd and Hoffman [38] experimentally investigated the heat transfer enhancement due to the spacer effect at subcritical condition. They found that heat transfer enhancement by space grid is similar to the enhancement of entrance effects in tube. Based on the research of spacer grids with blockage ratios varying from 0.25 to 0.35, Marek and Rehme [39] carried out the 3 rod bundle experiment cooled by air. They conducted the relation between the enhancement and the blockage ratio and found out that the heat transfer caused by space grids is directly related to the pressure drop through the spacer grids.

Based on Marek and Rehme's [39] experimental data in rod bundles, Yao et al. [40] developed the correlation in order to consider the heat transfer enhancement due to the spacer grids. Similar to the entrance effect, the enhancement becomes smaller with the distance to the space grids. For predicting the local enhancement and decay effect of spacer grids, the following form of correlation was proposed by Yao et al:

$$\frac{Nu}{Nu_\infty} = 1 + A\varepsilon^2 \exp(-B\frac{x}{D_h}) \quad (6)$$

**Table 9**
Correlations for spacer effect at subcritical condition.

| Authors | Correlations |
|---|---|
| Yao [38] | $\frac{Nu}{Nu_\infty} = 1 + 5.55\varepsilon^2 \exp(-0.13\frac{x}{D_h})$ |
| Holloway [39] | $\frac{Nu}{Nu_\infty} = 1 + 6.5\varepsilon^2 \exp(-0.8\frac{x}{D_h})$ |
| Miller [40] | $\frac{Nu}{Nu_\infty} = 1 + 465.4Re^{-0.5}\varepsilon^2 \exp(-7.31\times10^{-6}\times Re^{1.15}\frac{x}{D_h})$ |

where $\varepsilon$ is the blockage ratio caused by the space grids and x is the downstream distance to the exit of the spacer grid and $Nu_\infty$ represents the data without spacer effect. Yao gave the values of A=5.55 and B=0.13 as constant parameters in correlation (See Table 9) based on experiment data.

Holloway et al. [41] experimentally studied the heat transfer characteristics of 5 × 5 rod bundles with spacer effect at the condition of subcritical. Several kinds of spacer grids including simple spacer grid and spacer grid with split-vane were investigated. According to large number of experiment, correlation (See Table 9) for the local Nusselt numbers downstream of the simple spacer grid designs is developed based on the blockage.

Both the correlation of Yao and Holloway only considered the blockage ratio of spacer grid and the decay effect parameter as enhancement factor. However, Reynolds number, as an important parameter, was not considered. Mechanically speaking, the spacer grids affect the fluid flow because the thermal boundary layers were deprived by the spacer and must be redeveloped again downstream of the spacer. Similar to the entrance effect, the redevelopment increases the heat transfer in spacer grids downstream. Along with the distance downstream, this enhancement effect begins to decay within 20-40 times of hydraulics diameters. Out of the above range, heat transfer becomes normal, similar to bare rod without spacer effects.

Considering the Reynold number to the heat transfer enhancement, Miller et al. [42] conducted an experiment of enhancement heat transfer to 7 × 7 rod bundle at subcritical condition. In their experiment, all Reynolds number exceeds 5000, to ensure the fluid flows in turbulent region. They found that heat transfer enhancement reaches highest level at the point of spacer grid exit and such enhancement decays along with distance increase in downstream. In addition, they proved that the local Reynolds number, as well as the spacer blockage ratio and the downstream distance, strongly affect heat transfer enhancement both in spacer zone and in downstream decay zone. The correlation of Miller was listed in Table 9, considering the Reynolds number effect.

Moon et al. [43] conducted an experiment of 6 × 6 rod bundle at subcritical condition by single-phase steam cooling. The phenomenon of heat transfer enhancement was found in both upstream and downstream of spacer grids. In the downstream of the spacer, the heat transfer enhancement decays exponentially with the distance from the exit of the spacer grid. Their experimental data also showed that the Reynolds number enhances the heat transfer only at Reynolds number in lower range. For higher Reynolds numbers, the single-phase flow tends to restructure more quickly due to stronger turbulent mixing. The heat transfer enhancement by spacer grids may be lower than the effect by the turbulent flow. Therefore, with high Reynolds number, at their case greater than $10^4$, heat transfer enhancement by spacer grids can be treated to be independent of the Reynolds numbers.

### 4.2. Comparison with correlations with spacer effect

To evaluate the HT enhancement by spacer grid of the existing correlation developed at subcritical condition, comparison between experiment data (full databank and restricted databank) and correlations of Yao [38], Holloway [39] and Miller [40], which were also

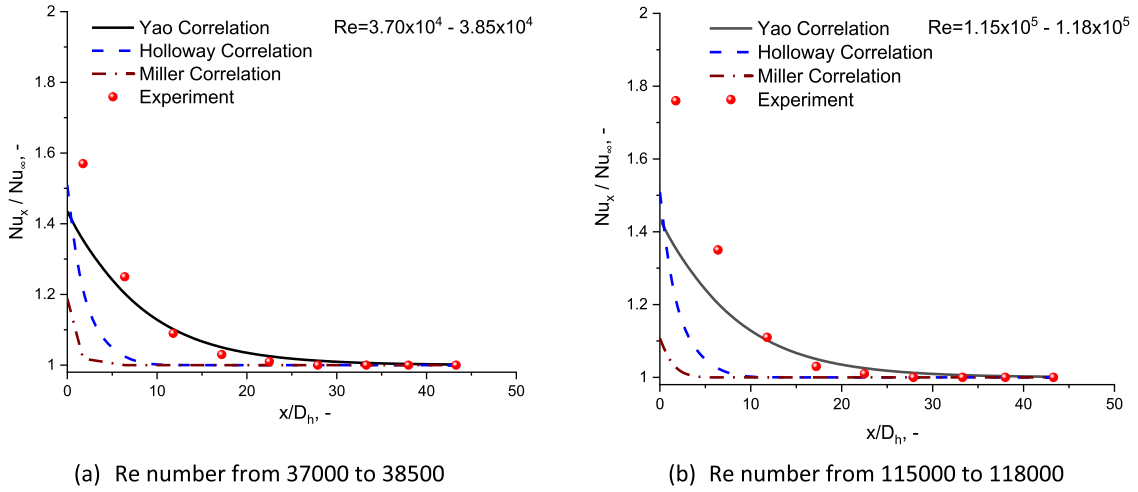


**Fig. 9.** Comparison between experiment and correlations of heat transfer enhancement.

**Table 10**
Mean deviation and standard deviation of Nu ratio.

| Correlations | $x/D_h \leq 5$ | | $5 < x/D_h \leq 10$ | | $10 < x/D_h \leq 20$ | |
|---|---|---|---|---|---|---|
| | $\mu$ | $\sigma$ | $\mu$ | $\sigma$ | $\mu$ | $\sigma$ |
| Yao [38] | -0.212 | 0.197 | -0.101 | 0.201 | -0.055 | 0.144 |
| Holloway [39] | -0.247 | 0.266 | -0.153 | 0.196 | -0.093 | 0.125 |
| Miller [40] | -0.305 | 0.311 | -0.178 | 0.187 | -0.087 | 0.107 |

developed by the similar simple spacer grid, were shown in Fig. 9 at the condition of two different mass flow rate.

Shown in Fig. 9, all the correlations underestimate the enhancement of heat transfer at supercritical condition. Among the three correlations, Yao correlation shows a good agreement with the decay tendency even though the maximum value of augmentation at the spacer outlet is significantly smaller than the experiment data. Compared experiment with different Re number, the level of heat transfer enhancement in high Re number is higher than that in low Re number. However, in Yao correlation, the heat transfer enhancement is only relevant to spacer design and the downstream location. So that the structure of Yao correlation should be modified with Re number in relevance.

The correlations of Holloway and Miller cannot follow the decay tendency. For Holloway correlation, the value of decay parameter -0.8 is too small and this leads to very quick decay for the enhancement. Similar to Holloway correlation, Miller correlation use Re both in augmentation term and decay term. In the case of large Re number, the enhancement of spacer grid totally disappears in 10 times of hydraulic diameter. This is not consistent with the current experimental result at supercritical condition because the enhancement due to the local effect at supercritical condition is much stronger than that at subcritical condition.

Table 10 shows the comparison Nu ratio calculated Correlation Yao, Holloway and Miller for decay effect from the test data of $x/D_h \leq 20$. From table 10, we can see that in the range of $x/D_h \leq 5$, the three correlations underestimate the Nu ratio, in other words, underestimate the enhancement value A at least 20 percent. With the increasing of $x/D_h$, the mean deviation and standard deviation reduced significantly. This is because the Nu ratios (both experiment and correlations) are converged to 1 with the increasing $x/D_h$. Seen from Fig. 9, the Nu ratios from both experiment and the correlations almost reach 1.0 when $x/D_h=20$ or larger value. So it is not necessary to investigate the validation of correlations at higher $x/D_h$ than 20 because the enhancement phenomenon decays to a very small value similar to normal heat transfer in fully-developed region.

The accuracies of Yao, Holloway and Miller correlations are not sufficient to predict the spacer effect at supercritical conditions. Therefore, a new correlation for supercritical water with spacer grid effect is expected to describe the enhancement heat transfer in supercritical cases.

### *4.3. Development of new heat transfer models for spacer effect in rod bundles*

Based on the full databank of supercritical water flowing in 2 × 2 rod bundles, a new heat transfer model for describing the effect of spacer grids on heat transfer at supercritical conditions was proposed under the following considerations:

(1) The quantity of heat transfer enhancement by spacer grid is dependent on both spacer grid design, i.e. blockage ratio, and flow parameters, i.e. Re number.
(2) The enhancement level is affected by the dimensionless downstream position and reaches the maximum at the exit of spacer grid.
(3) Strictly speaking, the decay effect is depended both on local positions ($x/D_h$) and Re number. However, literatures (e.g. Moon et al. [43]) proved that the effect caused by flow characteristics (Re number in present investigations) is much smaller than the local positions ($x/D_h$). In addition, for the easier structure of the predication correlations, the decay effect of local positions is no longer relevant to Re number, but only relevant to $x/D_h$.

According to the considerations above, the structure of the correlation to predicate the enhancement caused by space grid is shown as below

$$\begin{aligned} &\frac{Nu_x}{Nu_\infty} = f(\mathrm{Re}, x/D_h, \varepsilon) = 1 + A \times \varepsilon^2 \times e^{\left(-B\frac{x}{D_h}\right)} \\ &\mathrm{A} = f(\mathrm{Re}) \\ &\mathrm{B} = \mathrm{Const} \neq f(\mathrm{Re}, \varepsilon) \end{aligned} \tag{7}$$

Fig. 10(a), 10(b) and 10(c) show the measured Nu ratio versus Reynolds number at 3 fixed $x/D_h$ values of 1.7, 6.4 and 11.8. It can be seen that the effect of Re number to Nu ratio is rather small when the Re number is smaller than $1 \times 10^5$. In other words, a fixed value of Nu ratio can be used at Re number below $10^5$. With the increase of Re number from $10^5$, Nu ratio increases lineally with Re number and the higher fluid velocity contributes to the enhancement of heat transfer. Strictly speaking, all the data collected with different $x/D_h$ should be given to investigate the effect

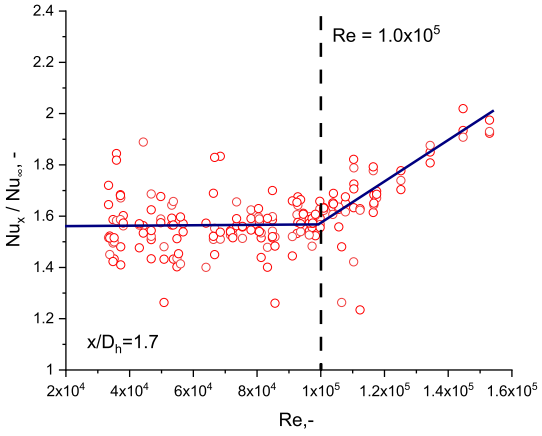


(c) Test data of fixed value of $x/D_h$=1.7

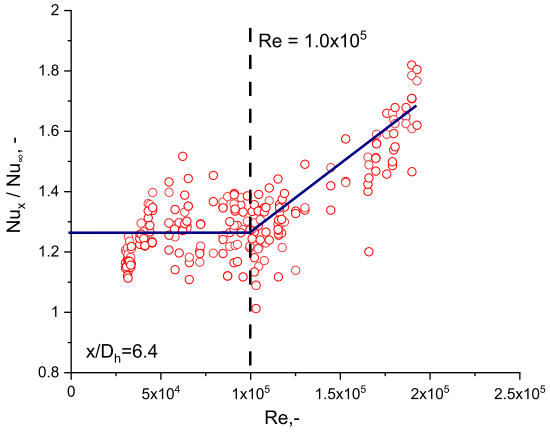


(d) Test data of fixed value of $x/D_h$=6.4

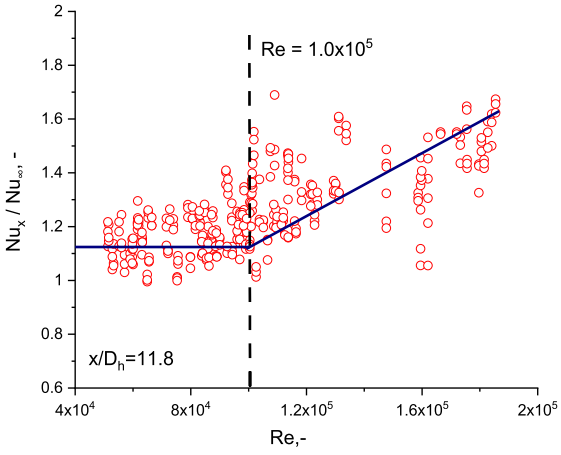


(e) Test data of fixed value of $x/D_h$=11.8

**Fig. 10.** Nu number ratio versus Re number at fixed $x/D_h$.

of Re number to Nu ratio. Because the heat transfer enhancement for high $x/D_h$ is significantly smaller than that in lower dimensionless position of $x/D_h$ and the tendency of them are quite similar to that of $x/D_h$ in Fig. 10. Thus, the comparison ot the larger $x/D_h$ is not shown in this paragraph specially.

The enhancement value A caused by spacer effect is strongly depended on Re number when Re number is larger than $1 \times 10^5$. To conduct the enhancement value A and the decay effect B, Re number should be fixed and the relation between $Nu_x/Nu_\infty$ and $x/D_h$ would be further investigate. Because of none-dependence of Re number lower than $10^5$, average $Nu_x/Nu_\infty$ data within this area can be obtained to fitting the decay parameter B of the correlation.

Fig. 11 shows the result of fitting line of decay effect B. In this fitting figure, averaged enhancement parameters by experiment at $x/D_h$ from 1.7 to 44 were selected. Experiment data of $x/D_h$=49.4 and 60.1 were not taken into consideration because the spacer effect at $x/D_h$>30 is not obvious. By extending the fitting line reversely and letting the fitting line reach the Y coordinates, parameter $A\varepsilon^2$ caused by flow acceleration as well as decay effect B can be also conducted with the following correlations.

$$\frac{Nu_x}{Nu_\infty} = 1 + A \times \varepsilon^2 \times e^{(-B\frac{x}{D_h})}$$
$$A\varepsilon^2 = 0.785 \ \ and \ \ \mathrm{B} = -0.21 \qquad (8)$$

It should be noted that correlation (8) was developed at Re<$10^5$ and whether it is valid at Re>$10^5$ should be further investigate. Fig. 12 shows the parameter $A\varepsilon^2$ for both test data with at Re<$10^5$ and with Re>$10^5$ from the full databank. It is clear that for test data with small Reynolds number Re < $10^5$, no significant dependence of the parameter $A\varepsilon^2$ on Reynolds number is observed. However, at large Reynolds number Re > $10^5$, an increase in parameter $A\varepsilon^2$ is obtained as Reynolds number increases, so that the following correlation is proposed:

$$\begin{aligned} A\varepsilon^2 &= 0.785 && if\ \mathrm{Re} \le 10^5 \\ &= 0.785 + 0.159 \times 10^{-4} \times (\mathrm{Re} - 10^5) && if\ \mathrm{Re} > 10^5 \end{aligned} \qquad (9)$$

In the present databank of 2 × 2 rod bundles with spacer grid effect, only two set of experiments with different blockage ratio were carried out in the investigations because it is hardly to design several types of space grids. For the research of blockage ratio to heat transfer enhancement, experiments data with more different blockage ratios are expected. It is well recognized by the community that the blockage ratio affects the enhancement is similar to that at sub-critical condition. Therefore, we validated the result obtained from the subcritical condition (e.g. Yao et al. [39] and Holloway et al. [40]) and assessed the conclusion that the enhancement value is proportional to blockage ratio with double power.

Fig. 13 compared the two different blockage ratio ($\varepsilon$=0.276 and 0.291) to the Nu ratio. For two blockage ratios, the heat transfer

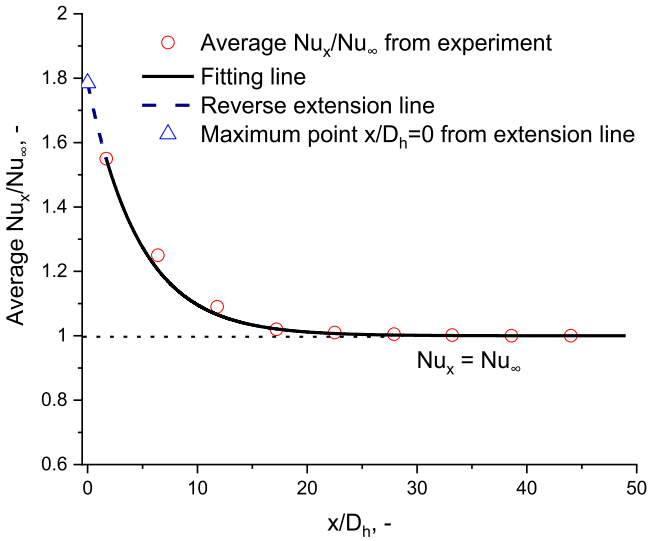


**Fig. 11.** Average Nu number ratio versus $x/D_h$ with Re number within $1 \times 10^5$.

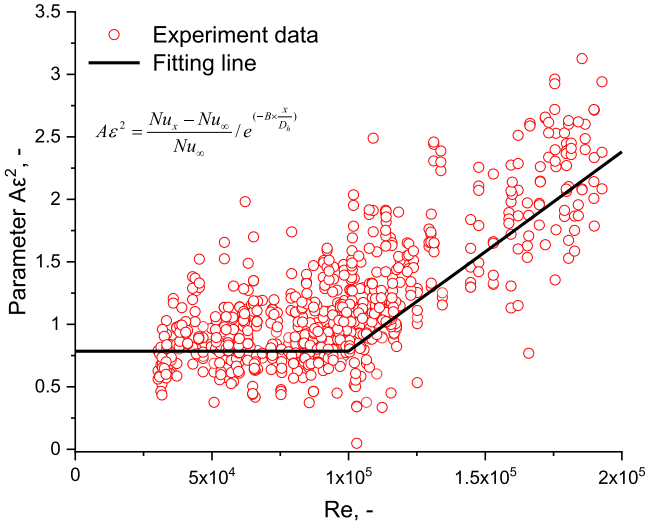


**Fig. 12.** Parameter$A\varepsilon^2$ versus the Re number of experiment data from full databank.

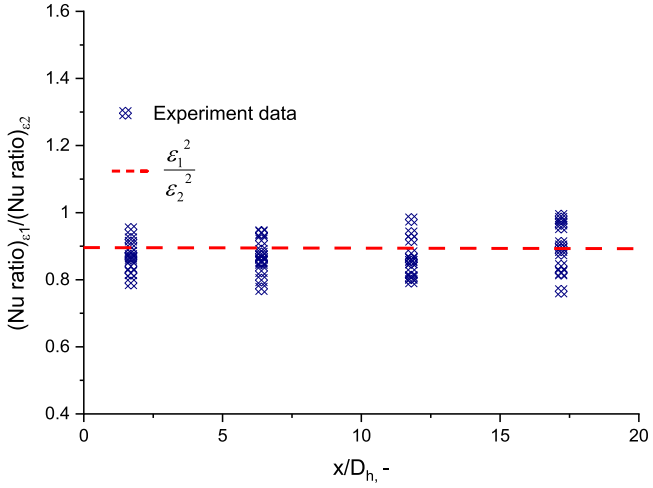


**Fig. 13.** Enhancement ratio with two spacer grids.

enhancement is nearly in direct proportion to the double power of the blockage ratio. We can refer that the results obtained from the subcritical condition can be also applied at supercritical condition. Considering the blockage ratio of spacer grid, the new correlation for spacer effect is summarized as below:

$$\begin{aligned} &\frac{Nu_x}{Nu_\infty} = 1 + A \times \varepsilon^2 \times e^{(-B\frac{x}{D_h})} \\ &A = 10.31 \qquad\qquad if\ \mathrm{Re} \le 10^5 \\ &\quad = 10.31 + 2.09 \times 10^{-4} \times (\mathrm{Re} - 10^5) \qquad if\ \mathrm{Re} > 10^5 \\ &\mathrm{B} = -0.21 \end{aligned} \tag{10}$$

### 4.4. Assessment of the new correlation

Fig. 14(a) and 14(b) show heat transfer ratio versus the distance from the spacer for selected test cases with Re<$10^5$ and Re>$10^5$. It can be seen that a good agreement is obtained for cases with both Reynolds number Re<$10^5$ and Re>$10^5$. Within the distance of 0-10 $x/D_h$ of downstream, new correlation can predict HT very well at lower Reynold number case and about 10% overestimate of Nu ratio within $10x/D_h$. So it can be referred that when the Re>$10^5$, the decay term B of the correlation (8) is still valid. Detail assessment result shows that the mean deviation μ and standard deviation $\sigma$ of the new correlation are 0.051 and 0.134 at the condition of $x/D_h \le 20$. Fig. 15 shows the mean deviation at different

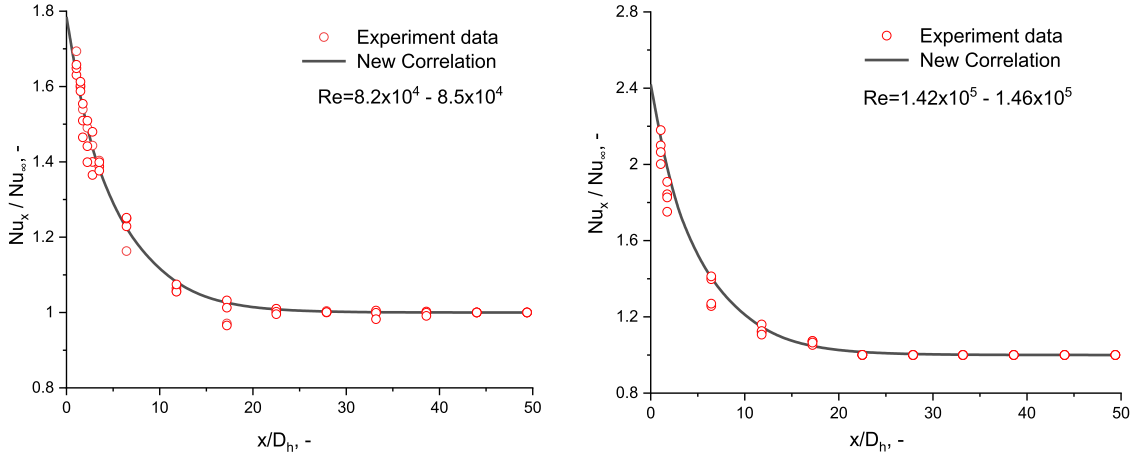


(a) Experiment cases of Re number from $8.2x10^4$ to $8.5x10^4$

(b) Experiment cases of Re number from $1.42x10^5$ to $1.46x10^5$

**Fig. 14.** Nu comparison of new developed model and experiment data.

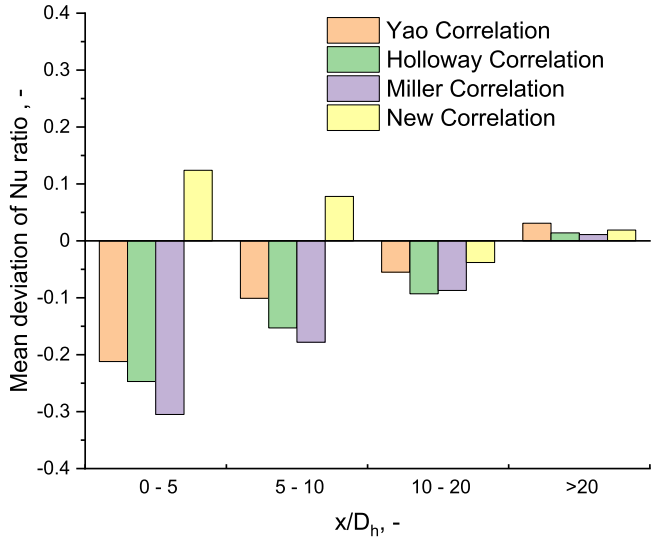


**Fig. 15.** Mean deviation μ at different $x/D_h$ ratio range.

$x/D_h$ ratio from Yao correlation, Holloway correlation, Miller correlation and new developed correlation. It is apparently that the accuracy of new correlation is significantly improved comparing with Yao, Holloway and Miller correlations, especially at short distance of spacer grid downstream.

## 5. Conclusions and outlook

In the present study, experiments of heat transfer in 2 × 2 rod bundles with spacer effect at supercritical conditions were carried out. The assessment of databank was done and the accuracy of heat transfer correlations to fully-developed region was indicated. In addition, a new heat transfer model about heat transfer enhancement by spacer effect was proposed. The following conclusions can be achieved:

(1) An experiment database of more than 5000 points were obtained. By checking the data quality and analyzing the databank, 3691 data points consists the full databank and 1042 data points consists the restricted databank because of lacking neighboring points. The combination of the full and restricted databanks can be adopted to assess the heat transfer models while only the full databank can be used to develop the new model.

(2) Model assessment work shows the Watts-Chou correlation can predict the heat transfer coefficient or Nu number without spacer effect accurately with 62.5% of data points within ±10% error band and 83.6% data points within ±20% error band.

(3) The existing correlations for predicting the heat transfer enhancement by spacer effect cannot be used in supercritical water because the large underestimating was observed at the exit of spacer grid. A new correlation with the similar structure of sub-critical correlations was proposed based on the databank of heat transfer at supercritical conditions.

(4) The new developed correlations with the spacer effect show satisfying accuracy and can predict the heat transfer enhancement due to the spacer grid effect. For the experiment data of $x/D_h \leq 20$, the mean and the standard deviation of the error parameter are 0.051 and 0.134.

Due to the limitation of the data in 2 × 2 rod bundles with spacer grids at supercritical conditions, all the correlation assessment and new model development are based on present experiment data. Nevertheless, our data can only provide 2 types of spacer grid and blockage ratio so that some assumptions (e.g. HT enhancement value is proportional to the spacer blockage ratio in double power) were made based on the knowledge of heat transfer in sub-critical cases. Therefore, the effects of different spacers for supercritical water heat transfer is still of interest in the future work.

## Credit author statement

Meng Zhao (M. Zhao): Writing- Original draft preparation, Experiment, Figure and Table

Fangnian Wang (F. N. Wang): Data reduction, Supervision

Aurelian Florin Badea (A.F. Badea): Consistent analyze of databank, Review and Editing.

## Declaration of Competing Interest

The authors declare that they have no known competing financial interests or personal relationships that could have appeared to influence the work reported in this paper.

## Acknowledgement

The authors would like to thank the German Federal Ministry for Economic Affairs and Energy (BMWi, VERA Project, No. 1501524) for providing the financial support for this study.

## References

[1] U.S. Department of EnergyA Technology Roadmap for Generation IV Nuclear Energy Systems, December 2002 Generation IV International Forum, GIF-002-00.
[2] I.L. Pioro, R.B. Duffey, Heat Transfer and Hydraulic Resistance at Supercritical Pressures in Power Engineering Applications, ASME Press, New York, 2007.
[3] I.L. Pioro, R.B. Duffey, Experimental heat transfer in supercritical water flow- ing inside channels (Survey), Nuclear Engineering and Design 235 (2005) 2407–2430 Vol.
[4] I.L. Pioro, H.F. Khartabil, R.B. Duffey, Heat transfer to supercritical fluids flow- ing in channels-empirical correlations (survey), Nuclear Engineering and De- sign 230 (2004) 69–91 Vol.
[5] X. Cheng, T. Schulenberg, Heat Transfer at Supercritical Pressure – Literature Review and Application to an HPLWR, Scientific Report FZKA 6609, Forschungszentrum Karlsuhe (May 2001).
[6] D. Huang, Z. Wu, B. Sunden, et al., A brief review on convection heat transfer of fluids at supercritical pressures in tubes and the recent progress, Applied Energy 162 (2016) 494–505 Vol.
[7] S. Koshizuka, N. Takano, Y. Oka, Numerical analysis of deterioration phenom- ena in heat transfer to supercritical water, International Journal of Heat and Mass Transfer 38 (1995) 3077–3084 Vol.
[8] K. Yamagata, K. Nishikawa, S. Hasegawa, et al., Forced convection heat trans- fer to supercritical water flowing in tubes, International Journals of Heat Mass Transfer 15 (1972) 2575–2593.
[9] P.L. Kirillov, A.N. Opanasenko, R.S. Pometko, et al., Experimental study of heat transfer on rod bundle at supercritical parameters of Freon-12, 2006 Federal Agency for Atomic Energy State scientific center of RF-Institute for physics and power engineering, FEI-3075, Obninsk, Russian.
[10] V.G. Razumovskiy, E.N. Pismennyy, A.E. Koloskov, et al., Heat Transfer to Super- critical Water in Vertical 7-Rod Bundles, 2008 16th International Conference on Nuclear Engineering (ICONE-16), Paper 48954, Orlando, Florida, USA, May 11-15.
[11] V.G. Razumovskiy, E.N. Pismennyy, A.E. Koloskov, et al., Heat Transfer to Super- critical Water in Vertical Annuli Channel and 3 Rod Bundles, 2009 17th Inter- national Conference on Nuclear Engineering (ICONE-17), Paper 75212, Brussels, Belgium, July 12-16.
[12] H. Mori, T. Kaida, M. Ohno, et al., Heat transfer to a supercritical pressure fluid flowing in sub-bundle channels, Journal of Nuclear Science and Technology 49 (2012) 373–383 Vol.
[13] B.V. Dyadyakin, A.S. Popov , Heat transfer and thermal resistance of tight sev- en-rod bundle, cooled with water flow at supercritical pressures, Trans. VTI (11) (1977) 244–253 in Russian.
[14] V.A. Silin, V.A. Voznesensky, A.M. Afrov, The light water integral reactor with natural circulation of the coolant at supercritical pressure B-500 SKDI, Nuclear Engineering and Design 144 (1993) 327–336 Vol.
[15] H. Wang, Q.C Bi., L.K. Leung, Heat transfer from a 2 × 2 wire-wrapped rod bundle to supercritical pressure water, International Journal of Heat and Mass Transfer 97 (2016) 486–501 Vol.

[16] H. Wang, Q.C Bi., L. Wang, et al., Experimental investigation of heat transfer from a 2 × 2 rod bundle to supercritical pressure water, Nuclear Engineering and Design 275 (2014) 205–218 Vol.
[17] L.K. Leung, A. Nava-Dominguez, Thermal-Hydraulics Program in Support of Canadian SCWR Concept Development, Journal of Nuclear Engineering and Ra- diation Science 4 (1) (2018) 011002 Vol.
[18] M. Ruzick, A. Vojac, T. Schulenberg, et al., European Project: Supercritical Water Reactor Fuel Qualification Test (SCWR-FQT): Overview, Results, Lessons Learnt and Future Outlook, Journal of Nuclear Engineering and Radiation Science 2 (2016) Vol, 011002–011001.
[19] H.Y. Gu, H.B Li, Z.X. Hu, et al., Heat transfer to supercritical water in a 2 × 2 rod bundle, Annals of Nuclear Energy 83 (2015) 114–124 Vol.
[20] H.Y. Gu, Z.X. Hu, D. Liu, et al., Experimental study on heat transfer to super- critical water in 2 × 2 rod bundle with wire wraps, Experimental Thermal and Fluid Science 70 (2016) 17–28 Vol.
[21] J. Kysela, R. Vsolak, O. Erben, in: Research Facilities of LVR-15 Research Reactor Research Facilities for the Future of Nuclear Energy, World Scientific Publishing Co., London, 1996, pp. 154–161. page.
[22] G. Heusener, U. Mueller, T. Schulenberg, et al., in: A European development program for a high performance light water reactor (HPLWR), Tokyo, 2000, pp. 23–28. Proceedings of SCR-2000pageNov.6-8.
[23] K.N. Song, K.H. Yoon, H.S. Kang, et al., Impact Analysis and Test on the Spacer Grid Assembly for PWRs, Key engineering materials 297 (2005) 1309–1314 Vol.
[24] Y. Xiao, J.L. Li, J. Deng, et al., Study of spacer effects on deteriorated heat trans- fer of supercritical fluid flow in an annulus, Progress in Nuclear Energy 123 (2020) 103306 Vol.
[25] M. Zhao, H.Y. Gu, X. Cheng, et al., Experimental and Numerical study on heat transfer of supercritical water flowing upward in 2 × 2 rod bundles, 2015 Pro- ceeding of 16th International Topical Meeting on Nuclear Reactor Thermal Hy- draulics (NURETH-16), Chicago, ILAugust 30-September 4.
[26] X. Cheng, M. Zhao, F. Feuerstein, et al., Prediction of heat transfer to supercrit- ical water at different boundary conditions, International Journal of Heat and Mass Transfer 131 (2019) 527–536 Vol.
[27] A.A. Bishop., R.O. Sandberg, L.S. Tong, Forced convection heat transfer to water at near-critical temperatures and supercritical pressures, Pittsburgh, USA, 1964 Report WCAP-2056, Part IV, Westinghouse Electric Corp..
[28] F.W. Dittus, L.M.K Boelter, in: Heat transfer in automobile radiators of the tubular type, University of California Press, Berkeley, 1930, pp. 443–461.
[29] H.S. Swenson, J.R. Caever, C.R. Kakarala, Heat Transfer to Supercritical Water in Smooth-Bore Tube, Journal of Heat Transfer 87 (1965) 477–484 Vol.
[30] M.J. Watts, C.T. Chou, Mixed convection heat transfer to supercritical pres- sure water, Proceedings of the Fourth International Heat Transfer Conference, München 3 (1982) 495–500 Vol.
[31] X. Cheng, Y.H. Yang, S.F. Huang, A simplified method for heat transfer pre- diction of supercritical fluids in circular tubes, Annals of Nuclear Energy 36 (2009) 1120–1128 Vol.
[32] J.D. Jackson, in: Consideration of the heat transfer properties of supercritical pressure water in connection with the cooling of advanced nuclear reactors, 2002 Proceedings of the 13th Pacific Basin Nuclear Conference, 21–25 October, Shenzhen City, China.
[33] P.L. Kirillov, Y. Yur'ev, V.P. Bobkov, et al., in: Handbook of Thermal-Hy- draulic Calculations, Energoa- tomizdat Publishing House, Moscow, Russia, 1990, pp. 66–67. Moscow, USSR(in Russian).
[34] Y.Y. Bae, H.Y. Kim, Convective heat transfer to CO2 at a supercritical pressure flowing vertically upward in tubes and an annular channel, Experimental Ther- mal and Fluid Science 33 (2009) 329–339 Vol.
[35] A.H. Harvey, D.G. Friend, Aqueous Systems at Elevated Temperatures and Pres- sures- Chapter 1: Physical Properties of water, Physical Chemistry in Water, Steam and Hydrothermal Solutions (2004) 1–27.
[36] Y.Y. Bae, H.Y. Kim, T.H. Yoo, Effect of a helical wire on mixed convection heat transfer to carbon dioxide in a vertical circular tube at supercritical pressures, International Journal of Heat and Fluid Flow 32 (2011) 340–351 Vol.
[37] H. Wang, Q.C. Bi, Z.D. Yang, et al., Experimental and numerical study on the enhanced effect of spiral spacer to heat transfer of supercritical pressure water in vertical annular channels, Applied Thermal Engineering 48 (2012) 436–445 Vol.
[38] G.J. Kidd, H.W. Hoffman, The Temperature Structure and Heat Transfer Charac- teristics of an Electrically Heated Model of a Seven-Rod Cluster Fuel Element, 1968 ASME Paper 68-WA/HT-33.
[39] J. Marek, K. Rehme, Heat transfer in smooth and roughened rod bundles near spacer grids, 1975 Kernforschungszentrum Karlsruhe (F.R. Germany), Report No. KFK-2128(in German).
[40] S. Yao, L. Hochreiter, W. Leech, Heat transfer augmentation in rod bundles near grid spacers, Journal of Heat Transfer 104 (1982) 76–81 Vol.
[41] M.V. Holloway, H.L. McClusky, D.E. Beasley, The Effect of Support Grid Features on Local, Single-Phase Heat Transfer Measurements in Rod Bundles, Journal of Heat Transfer 126 (2004) 43–53 Vol.
[42] D.J. Miller, F.B. Cheung, S.M. Bajorek, On the development of a grid enhanced single-phase convective heat transfer correlation, Nuclear Engineering and De- sign 264 (2013) 56–60 Vol.
[43] S.K. Moon, J. Kim, S. Cho, et al., Single-phase convective heat transfer enhance- ment by spacer grids in a rod bundle, Journal of Nuclear Science and Technol- ogy 51 (2014) 543–557 Vol.